Phosphorylation of Ser-204 and Tyr-405 in human malonyl-CoA decarboxylase expressed in silkworm Bombyx mori regulates catalytic decarboxylase activity

Phosphorylation of Ser-204 and Tyr-405 in human malonyl-CoA decarboxylase expressed in silkworm *Bombyx mori* regulates catalytic decarboxylase activity

In-Wook Hwang · Yu Makishima · Tomohiro Suzuki · Tatsuya Kato · Sungjo Park · Andre Terzic · Shin-kyo Chung · Enoch Y. Park

---

In-Wook Hwang · Enoch Y. Park (✉)
Laboratory of Biotechnology, Integrated Bioscience Section, Graduate School of Science and Technology, Shizuoka University, 836 Ohya, Suruga-ku, Shizuoka, 422-8529, Japan. E-mail: park.enoch@shizuoka.ac.jp; Tel. & Fax: +81-54-2384887

Yu Makishima · Tatsuya Kato · Enoch Y. Park
Laboratory of Biotechnology, Department of Applied Biological Chemistry, Faculty of Agriculture, Shizuoka University, 836 Ohya, Suruga-ku, Shizuoka, 422-8529, Japan.

Tomohiro Suzuki
Research Institute of Green Science and Technology, Shizuoka University, 836 Ohya Suruga-ku, Shizuoka, 422-8529, Japan.

Tatsuya Kato · Enoch Y. Park
Laboratory of Biotechnology, Green Chemistry Research Division, Research Institute of Green Science and Technology, Shizuoka University, 836 Ohya Suruga-ku, Shizuoka, 422-8529, Japan.

Sungjo Park · Andre Terzic
Center for Regenerative Medicine, Mayo Clinic, 200 First Street SW, Rochester, MN, 55905, USA. Marriott Heart Disease Research Program, Division of Cardiovascular Diseases, Departments of Medicine, Molecular Pharmacology and Experimental Therapeutics, and Medical Genetics, Mayo Clinic, 200 First Street SW, Rochester, MN, 55905, USA.

Shin-kyo Chung
School of Food Science and Biotechnology, Kyungpook National University, Daegu 702-701, Republic of Korea

Authors' E-mail address;
In-Wook Hwang: gunryung21@hanmail.net (IH)
Yu Makishima: mmm.yu@live.jp (YM)
Tomohiro Suzuki: atsuzuk@ipc.shizuoka.ac.jp (TS)
Tatsuya Kato: atkato@ipc.shizuoka.ac.jp (TK)
Sungjo Park: park.sungjo@mayo.edu (SP)
Andre Terzic: terzic.andre@mayo.edu (AT)
Shin-kyo Chung: kchung@knu.ac.kr (SC)
Enoch Y. Park: park.enoch@shizuoka.ac.jp (EYP)

ABSTRACT

Decarboxylation of malonyl-CoA to acetyl-CoA by malonyl-CoA decarboxylase (MCD; EC 4.1.1.9) is a vital catalytic reaction of lipid metabolism. While it is established that phosphorylation of MCD modulates the enzymatic activity, the specific phosphorylation sites associated with the catalytic function have not been documented due to lack of sufficient production of MCD with proper post-translational modifications. Here, we used the silkworm-based BmNPV bacmid system to express human MCD (hMCD) and mapped phosphorylation effects on enzymatic function. Purified MCD from silkworm displayed post-translational phosphorylation and demonstrated coherent enzymatic activity with high yield (~200 µg/silkworm). Point mutations in putative phosphorylation sites, Ser-204 or Tyr-405 of hMCD, identified by bioinformatics and proteomics analyses reduced the catalytic activity, underscoring the functional significance of phosphorylation in modulating decarboxylase-based catalysis. Identified phosphorylated residues are distinct from the decarboxylation catalytic site, implicating a phosphorylation-induced global conformational change of MCD as responsible in altering catalytic function. We conclude that phosphorylation of Ser-204 and Tyr-405 regulates the decarboxylase function of hMCD leveraging the silkworm-based BmNPV bacmid expression system that offers a fail-safe eukaryotic production platform implementing proper post-translational modification such as phosphorylation.

Keywords Human malonyl-CoA decarboxylase (hMCD) · Site directed mutagenesis · Phosphorylation/dephosphorylation · Lipid metabolism · Silkworm · *Bombyx mori* nucleopolyhedrovirus

Introduction

Malonyl-CoA decarboxylase (MCD, E.C.4.1.1.9), encoded by *MLYCD*, is the crucial metabolic enzyme responsible for sustaining homeostatic lipid metabolism (Dyck et al. 2006; Folmes et al. 2013; Saggerson 2008). Due to the importance of cellular functions in fatty acid metabolism, MCD is ubiquitously expressed in all living organisms locating in mitochondria, peroxisome and cytoplasm (Buckner et al. 1976; Kim et al. 1979; Scholte 1969). In humans, deficiency of MCD (OMIM 248360) precipitates a spectrum of disorders including cardiomyopathy, hypoglycaemia, hypotonia, mild mental retardation, metabolic acidosis, malonic aciduria, seizures and vomiting (Brown et al. 1984; Haan et al. 1986; Krawinkel et al. 1994; MacPhee et al. 1993; Matalon et al. 1993; Xue et al. 2012; Yano et al. 1997).

MCD participates in the degradation of malonyl-CoA, an integral metabolic intermediate in anabolic/catabolic lipid metabolism (Figures S1 and S2, Supporting Information). Malonyl-CoA is a committed substrate for *de novo* fatty acid biosynthesis, yet abundant malonyl-CoA inhibits carnitine palmitoyltransferase 1 (CPT-1), a rate-limiting step for long-chain fatty acid transport into mitochondria and subsequent lipid β-oxidation (Kim et al. 1989; Pender et al. 2006). Inhibition of MCD reduces fatty acid β-oxidation and accelerates glucose oxidation, producing a metabolic switch in energy substrate preference (Dyck et al. 2006). Consequently, regulation of MCD activity to modulate intracellular malonyl-CoA levels is considered for potential therapeutic applications to mitigate metabolic disorders.

Post-translational modification of MCD modulates enzymatic function (Dyck et al. 2000; Laurent et al. 2013; Park et al. 2002; Saha et al. 2000; Sambandam et al. 2004; Voilley et al. 1999). For example, MCD has several acetylation sites and MCD deacetylation inhibits the decarboxylase activity thereby promoting *de novo* lipogenesis, whereas MCD acetylation

enhances fatty acid oxidation (Laurent et al. 2013). In contrast, the catalytic activity associated with MCD phosphorylation/dephosphorylation has not been definitively documented as phosphorylation sites have not been identified and production of sufficient authentic MCD with suitable post-translational modification remains limited (Dyck et al. 2000; Park et al. 2002; Saha et al. 2000; Sambandam et al. 2004; Voilley et al. 1999).

The *E. coli* expression system has been widely used for recombinant protein production, yet the proteins expressed in this system often show poor post-translational modifications (Kamionka 2011). To secure genuine eukaryotic protein production with proper post-translational modifications, a *Bombyx mori* nucleopolyhedrovirus (BmNPV) bacmid, a hybrid shuttle vector for an *E. coli* and *B. mori*, has been developed (Kato et al. 2010; Motohashi et al. 2005). With this system, we have successfully produced cellular, mitochondrial, and membrane proteins with proper folding and post-translational modifications (Figure S3, Supporting Information) (Dojima et al. 2009; Du et al. 2009; Hwang et al. 2014).

Here, we examined whether phosphorylation of human MCD (hMCD) generated using the silkworm-based BmNPV bacmid expression system modulates the essential decarboxylase activity. We report that the recombinant hMCD displays phosphorylation properties with consistent catalytic activity. Point mutations in the phosphorylation sites, namely Ser-204 and Tyr-405, limit the enzymatic activity of hMCD, underscoring the regulation of catalytic function by phosphorylation. The silkworm-based BmNPV bacmid expression system thus provides a reliable recombinant eukaryotic protein production modality with proper post-translational phosphorylation suitable for functional analysis of human MCD.

Materials and Methods

Construction of recombinant Δ39aa-hMCD BmNPV bacmid and mutants

The overall strategy for the construction and expression of Δ39aa-hMCD BmNPV bacmid is shown in Figure 1. The complementary DNA of hMCD from Mammalian Gene Collection (GenBank EAW95513.1, Thermo Scientific, Pittsburgh, PA, USA) was used as a template. N-terminal 39 amino acids of hMCD, a putative mitochondria targeting sequence, were deleted using conventional polymerase chain reaction (PCR) with a pair of primers containing the *Bam*HI/*Xho*I restriction cloning site: 5′-GCGGATCCCACCATGGACTACAAGGATGACGATGACAAGATGGACGAGCTGCTGCGCCGC-3′ (forward), 5′-GCCTCGAGTCAGAGCTTGCTGTTCTTTTGAAACTG-3′ (reverse). Deletion of the mitochondria targeting sequence leads to high protein expression and does not affect the enzyme activity (Zhou et al. 2004). In addition, the Kozak consensus sequence and the FLAG tag sequence were attached at N-terminus for high expression levels in baculovirus expression system and for purification of expressed protein, respectively. The PCR cycle was conducted following 40 cycles of denaturation at 98°C for 10 s, annealing at 55°C for 5 s, and extension at 72°C for 10 s using PrimeSTAR® Max premix kit (Takara Bio Inc., Otsu, Shiga, Japan). The resultant PCR product (Δ39aa-hMCD gene) was digested with *Bam*HI and *Xho*I followed by purification with a GFX™ PCR DNA and Gel Band Purification Kit (GE Healthcare, Amersham, UK). The purified DNA fragment was ligated into pFastbac 1 vector, transformed into *E. coli* competent DH5α cells (Invitrogen, Carlsbad, CA, USA) and then cultured on a solid LB medium containing 100 μg/mL of ampicillin at 37°C for 18 h. The plasmid containing Δ39aa-hMCD gene was isolated and its sequence identity was confirmed by DNA sequencing. Finally, *E. coli* BmDH10bac-*CP*⁻-*Chi*⁻ competent cells containing the cysteine proteinase- and chitinase-deficient BmNPV bacmid (Park et al. 2008a) were transformed with the pFastbac1-Δ39aa-hMCD and cultured on a solid LB medium containing 50 μg/mL of kanamycin, 7 μg/mL of gentamycin, 10 μg/mL of tetracycline, 40 μg/mL of isopropyl β-D-1-thiogalactopyranoside (IPTG) and 100 μg/mL of

5-bromo-4-chloro-3-indolyl-4-galactoside (X-Gal) (Takara Bio) at 37°C for 18 h (Figure S4, Supporting Information). To confirm the BmNPV-Δ39aa-hMCD, bacmid PCR of white colonies was assessed using M13 primers. The PCR cycle was conducted following 30 cycles of denaturation at 98°C for 10 s, annealing at 55°C for 10 s, and extension at 72°C for 40 s using SapphireAmp Fast PCR Master Mix kit (Takara Bio). The recombinant BmNPV bacmid (BmNPV-Δ39aa-hMCD) was isolated from positive colonies confirmed by bacmid PCR.

For the construction of mutated hMCD BmNPV bacmid (S204G and Y405F), the QuikChangeII XL Site-Directed Mutagenesis Kit (Stratagene, La Jolla, CA, USA) was used according to the manufacturer's protocols. The pFastbac-Δ39aa-hMCDs containing the desired mutation were produced using the constructed pFastbac-Δ39aa-hMCD as a template by PCR reaction with primer sets containing changed base for mutation: 5′-GGGTTACCTGGCATGGACCGTGTGAAGTGCTTC-3′ (forward primer for S204G), 5′-GAAGCACTTCACACGGTCCATGCCAGGTAACCC-3′ (reverse primer for S204G), 5′-AGGCTGTGCGCCTGGTTCCTGTATGGAGAGAAG-3′ (forward primer for Y405F), 5′-CTTCTCTCCATACAGGAACCAGGCGCACAGCCT-3′ (reverse primer for Y405F). The PCR cycle was conducted following 18 cycles of denaturation at 95°C for 15s, annealing at 60°C for 30s, and extension at 68°C for 6.5 min. After *Dpn* I treatment at 37°C for 3 hr, *Dpn* I-treated plasmids were transformed into XL10-Gold ultracompetent cells (Stratagene). The plasmid containing pFastbac-Δ39aa-hMCD mutant genes were isolated and its sequence identity with mutation was confirmed by DNA sequencing.

Expression and purification of recombinant Δ39aa-hMCD in silkworm larvae and pupae

To produce a recombinant protein in silkworm, 10 μg of each recombinant BmNPV bacmid DNA was directly injected with DMRIE-C reagent (Invitrogen) into the dorsum of larvae and

159 pupae using a syringe with a 26-gauge beveled needle (Terumo Co. Tokyo, Japan). The
160 injected larvae and pupae were reared at 27°C in an incubator for 6–7 days. In the case of
161 larvae, the fat body was collected by cutting and dissection. The samples including fat body
162 or pupae were immediately frozen at –80°C until further analysis. Protein purification was
163 carried out at 4°C to minimize aggregation and protease activity. The aliquot of collected
164 larval fat body or pupae was homogenized in 10 mL of lysis buffer (50 mM Tris-HCl, 150
165 mM NaCl, pH 7.4 and 0.1% TritonX-100) containing an EDTA-free protease inhibitor tablet
166 (Roche, Mannheim, Germany) using a homogenizer (GLH-115, Yamato, Tokyo, Japan). Cell
167 debris was removed by pelleting through centrifugation at 12,000 *g* for 30 min. The
168 supernatant was filtered using a 0.45 μm syringe filter and loaded onto a 500 μL of anti-
169 FLAG M2 antibody affinity gel (Sigma-Aldrich, St. Louis, MO, USA) pre-equilibrated with
170 equilibration buffer (50 mM Tris-HCl, 150 mM NaCl, pH 7.4 and 0.02% TritonX-100). The
171 column was washed with 2.5 mL of equilibration buffer and eluted with elution buffer (100
172 μg/mL FLAG peptide in 50 mM Tris-HCl and 150 mM NaCl, pH 7.4). Purified protein
173 concentration was determined using BCA protein assay kit (Thermo Scientific, Rockford, IL,
174 USA).

175 SDS-PAGE and Western blotting

176 The integrity of purified Δ39aa-hMCD was determined by Coomassie brilliant blue (CBB)-
177 staining and western blotting analyses (Karger et al. 2008; Park et al. 2008b). Prior to
178 electrophoresis, purified samples were boiled for 5 min at 95°C with protein denaturing
179 buffer (Nacalai Tesque, Kyoto, Japan). Samples were electrophoresed in a 10% sodium
180 dodecyl sulfate polyacrylamide gel electrophoresis (SDS-PAGE) gel with a Mini-protean
181 system (Bio-Rad, Hercules, CA, USA) at 150 V for 45–60 min in Tris-glycine buffer (25 mM
182 Tris, 250 mM glycine, pH 8.3 and 0.1% SDS). After electrophoresis, the SDS-PAGE gel was

183 stained with Coomassie blue staining solution. For Western blotting analysis, the separated
184 proteins on a SDS-PAGE gel were transferred to PVDF membranes (GE Healthcare) by
185 electroblotting on a semi-dry blotter (Bio-Rad) at 15 V for 1 h. To detect the purified Δ39aa-
186 hMCD and their phosphorylation, a mouse anti-FLAG antibody (Wako Pure Chem. Ind. Ltd.,
187 Osaka, Japan), anti-phosphoserine antibody and anti-phosphotyrosine (Sigma-Aldrich) were
188 used as primary antibodies, respectively. An anti-mouse IgG-HRP (GE Healthcare) was used
189 as a secondary antibody in both cases.

190 MCD activity assay

191 The hMCD activity was measured by the production of NADH in the coupled reactions (Kim
192 and Kolattukudy 1978). The NADH is accumulated by the reaction of acetyl-CoA from
193 malonyl-CoA and oxaloacetate from malate (Eqs. 1–3).

194 $$\text{Malonyl} - \text{CoA} \xrightarrow{\text{Malonyl-CoA decarboxylase}} \text{Acetyl} - \text{CoA} + CO_2 \qquad (1)$$

195 $$\text{Malate} + \text{NAD} \xleftrightarrow{\text{Malate dehydrogenase}} \text{Oxaloacetate} + \text{NADH} \qquad (2)$$

196 $$\text{Acetyl} - \text{CoA} + \text{Oxaloacetate} \xrightarrow{\text{Citrate synthase}} \text{Citrate} + \text{CoA} \qquad (3)$$

197 To measure the decarboxylase activity of recombinant hMCD, 10 μg of purified Δ39aa-
198 hMCD was incubated with 36 μL of reaction buffer (10 mM of Tris-HCl, pH 7.5, 2 mM of
199 malate, 2 mM of NAD, 0.8 U of malate dehydrogenase) at room temperature. After 5 min,
200 assay was initiated by the addition of 3 mM of malonyl-CoA and incubated at 37°C. After 10
201 min, 0.03 U of citrate synthase was added to the incubated solution. The reaction was
202 terminated by addition of 4 μL of 100% trichloroacetic acid. The produced NADH during
203 reaction was detected using an UV-visible spectrophotometer by measuring the absorbance at
204 340 nm.

205 **Results**

206 Expression and purification of Δ39aa-hMCD

207 The hMCD harbors a mitochondrial targeting sequence (39 amino acids) at N-terminus and a
208 peroxisomal targeting sequence (Ser-Lys-Leu, SKL) at C-terminus (Fig. 1). The peroxiomal
209 SKL residues do not affect the protein expression levels, but the mitochondrial targeting
210 sequence significantly diminishes MCD expression (Voilley et al. 1999). Therefore, we
211 designed a construct without a mitochondrial targeting sequence but retaining the
212 peroxisomal SKL sequence to enhance the recombinant hMCD production (Fig. 1). The
213 recombinant Δ39aa-hMCD with an N-terminal FLAG tag was expressed in silkworm larvae
214 and pupae, and purified using an anti-FLAG M2 affinity gel column. The purified Δ39aa-
215 hMCD protein with more than 95% purity migrated to ~50 kDa, an estimated molecular
216 weight on SDS-PAGE based on comparison with molecular weight markers (Fig. 2A).
217 Western blot analysis using a FLAG-specific antibody confirmed the specific expression of
218 Δ39aa-hMCD (Fig. 2B). In mock-injected silkworm, however, hMCD bands were not
219 detected in both fat body and pupae samples (Fig. 2B). Thus, the recombinant Δ39aa-hMCD
220 purified here demonstrated significant homogeneity suitable for biochemical and functional
221 analyses.

222 Silkworm-based recombinant protein expression conventionally provides a high yield of
223 purified proteins in the range of 20 – 500 μg/silkworm (Table 1). Consistent with this, the
224 average yields of purified Δ39aa-hMCD from ten silkworm larvae and five pupae were 119
225 μg/larva and 344 μg/pupa. The pupae-based protein expression provided a higher yield of
226 purified protein than the fat body-based expression, probably due to the difference of organ
227 size and protease activity in the expression host. Specific decarboxylase activities of the
228 purified Δ39aa-hMCD, measured by the production of NADH in the coupled reactions, were

229 59.54 ± 7.68 (n = 6) nmol/mg/min from silkworm fat body and 48.16 ± 7.89 (n = 6)
230 nmol/mg/min from silkworm pupae (Table 2). These measured enzymatic activities showed
231 no significant statistical difference (p>0.05), but are much higher than that of human
232 recombinant MCD purified from *E. coli* (Zhou et al. 2004) indicating that the post-
233 translational modifications implemented in silkworms regulate catalytic activity.

234 Phosphorylation-induced catalytic function of Δ39aa-hMCD

235 The catalytic activity of MCD associated with phosphorylation/dephosphorylation was
236 previously evaluated (Dyck et al. 1998; Park et al. 2002; Saha et al. 2000), yet these studies
237 provided inconsistent results either a decrease or increase in decarboxylase activity of MCD.
238 To clarify the phosphorylation-induced effects on MCD enzymatic function, potential
239 phosphorylation sites of hMCD were examined. NetPhos 2.0, neural network predictions for
240 serine, threonine and tyrosine phosphorylation in eukaryotic proteins
241 (http://www.cbs.dtu.dk/services/NetPhos/), was applied to predict hMCD phosphorylation
242 sites (Blom et al. 1999) (Fig. 3A). Four serine (Ser-204, Ser-275, Ser-326, Ser-380), four
243 threonine (Thr-9, Thr-60, Thr-245, Thr-396) and one tyrosine (Tyr-468) residues were
244 putatively identified as phosphorylation sites, which are well conserved (Fig. 3A & 3B).
245 Typically, each phosphorylation prediction program maps slightly different potential amino
246 acid residues depending on bioinformatics algorithm. Based on the NetPhos 2.0 prediction
247 with 9 amino acid residues as potential phosphorylation sites, we performed the mass
248 spectrometry analysis to narrow down the proteomic search, and identified exclusive
249 phosphorylation of Ser-204 and Tyr-405 in the recombinant Δ39aa-hMCD, thereby excluding
250 the investigation of other predicted phosphorylation sites. Accordingly, these residues were
251 mutated to glycine (S204G) and phenylalanine (Y405F) using site-directed mutagenesis to
252 eliminate the hydroxyl group for phosphorylation (Fig. 3C).

253 The point mutants S204G and Y405F were purified from silkworm fat body and pupae,
254 and analyzed by Western blotting using an anti-phosphoserine and anti-phosphotyrosine
255 antibodies (Fig. 4). The Δ39aa-hMCD mutants displayed a substantial decrease on Western
256 blotting analysis compared with the wild type Δ39aa-hMCD, indicating that Ser-204 and Tyr-
257 405 are indeed the residues for phosphorylation. The lack of complete absence of the
258 phosphorylated MCD band in Western blotting, however, could be ascribed to phosphorylated
259 amino acid residues other than Ser-204 and Tyr-405.

260 To evaluate the effect of phosphorylation on the biological function of hMCD, the
261 decarboxylase activity of Δ39aa-hMCD mutants were measured. The specific activities of
262 S204G mutant purified from fat body and pupae were 30.36 ± 2.25 (n = 6) and 24.37 ± 1.99
263 nmol/mg/min (n = 6), respectively, which are lower by 50% than that of wild type Δ39aa-
264 hMCD (Table 3). In addition, the specific activities of Y405F mutants were 33.45 ± 3.56 (n =
265 6) and 31.24 ± 1.69 nmol/mg/min (n = 6) purified from fat body and pupae, respectively.
266 Collectively, the dephosphorylation of hMCD diminishes decarboxylase activity, underlining
267 the phosphorylation-induced regulation in catalytic function.

268 Structural implication of hMCD phosphorylation

269 The resolved crystal structure of hMCD (PDB accession number: 4F0X) reveals a molecular
270 tetramer, composed by a dimer of structural heterodimer where the two subunits show
271 different conformations (Fig. 5) (Aparicio et al. 2013). The monomer of MCD has an N-
272 terminal helical domain for oligomerization and a C-terminal domain for catalysis, and the
273 active site of MCD is located in a prominent groove clustered with evolutionarily conserved
274 residues (Fig. 5A) (Aparicio et al. 2013; Froese et al. 2013). Through inter-subunit disulfide
275 bonds, Cys-206—Cys-206 and Cys-243—Cys-243 (Fig. 5B), the four subunits of the
276 tetramer are connected, providing positive cooperativity to the decarboxylase catalytic

277 function (Aparicio et al. 2013).

278 Ser-204 identified here for the phosphorylated residue is located in the beginning of the
279 catalytic domain. The side chain of Ser-204 is fully exposed to solvent in the monomeric
280 structure (Fig. 5A & 5C), and ~20 Å away from the active site, suggesting that the
281 phosphorylation could not directly affect the structural integrity of the catalytic active site.
282 However, the quaternary structure of hMCD reveals that Ser-204 is located nearby the Cys-
283 206, the essential residue for the inter-subunit disulfide bond interaction (Fig. 5C). Thus, the
284 phosphorylation/dephosphorylation of Ser-204 might modulate the disulfide bridge formation,
285 contributing to the catalytic function. Moreover, as Lys-210 (rat sequence; Lys-211 in human)
286 has been reported to be an essential amino acid residue for rat MCD enzymatic function
287 through acetylation (Nam et al. 2006), the post-translational modifications in the vicinity of
288 Cys-206 could be a key player in regulation of MCD function.

289 In contrast to Ser-204, Tyr-405 is not in the vicinity of inter-subunit interactions. This
290 residue is located near to the catalytic dyad with His-423 and Ser-329. The hydroxyl group of
291 Tyr-405 forms a hydrogen bond with the side chain of Asn-417, which is in the same α-helix
292 harboring catalytic His-423 (Fig. 5D). Based on this structural information, the
293 phosphorylation of Tyr-405 might induce the conformational change of a catalytic dyad
294 producing the fine-tuning in decarboxylase activity.

295 **Discussion**

296 Malonyl-CoA decarboxylase is a metabolic enzyme participating in the production of acetyl-
297 CoA from malonyl-CoA, a vital metabolite for anabolic fatty acid biosynthesis and catabolic
298 lipid oxidation (Dyck et al. 1998; Pender et al. 2006). MCD overexpression increases fatty
299 acid oxidation and improves whole body insulin resistance (An et al. 2004), whereas reduced
300 MCD levels decrease lipid oxidation with an increase in glucose oxidation in human

301 myotubes (Bouzakri et al. 2008). In addition, catalytic function of MCD is regulated by
302 multiple factors including post-translational modifications (Dyck et al. 2000; Nam et al.
303 2006; Park et al. 2002; Saha et al. 2000). Due to the pathophysiological relevance of MCD in
304 metabolism-associated disorders, the regulation of MCD activity has been increasingly
305 recognized as a candidate target for therapeutic interventions, essentially requiring authentic
306 heterologous protein production to map critical molecular entities (Sambandam et al. 2004;
307 Saggerson 2008). Here, we successfully produced recombinant hMCD using the silkworm-
308 based BmNPV expression system equipped with a proper post-translational modification
309 machinery. The heterologous MCD from silkworm demonstrated an essential and higher
310 decarboxylase activity compared to that of MCD from *E. coli* (Zhou et al. 2004),
311 underscoring the enzymatic activity enhancement by post-translational modifications
312 implemented in silkworm. Furthermore, we identified two critical phosphorylated residues of
313 Ser204 and Tyr-405 involved in regulation of decarboxylase-based catalysis.

314 AMP-activated protein kinase (AMPK) has been suggested to regulate MCD activity.
315 Phosphorylation of MCD by AMPK promotes the enzymatic activity, leading to a decrease in
316 the malonyl-CoA levels, whereas dephosphorylation inhibits the catabolic function (Park et al.
317 2002; Saha et al. 2000). Up to date, several putative phosphorylation sites on serine,
318 threonine and tyrosine residues have been suggested, (Voilley et al. 1999), yet critical
319 phosphorylation residues affecting the human MCD activity have remained elusive. By
320 utilizing bioinformatics and mass spectrometry analyses, we identified exclusive
321 phosphorylation of Ser-204 and Tyr-405. Point mutations of the phosphorylation sites
322 decreased specific activity of hMCD, highlighting the biological significance of Ser-204 and
323 Tyr-405 in regulating decarboxylase activity.

324 In summary, silkworm-based BmNPV protein expression system successfully produced
325 the human MCD with high yield and post-translation modification. Heterologous MCD

326 retains essential decarboxylase activity and harbors two post-translational phosphorylation
327 residues, namely Ser-204 and Tyr-405, critical in modulating MCD catalytic function.
328 Identified phosphorylated residues are distinct from the decarboxylation catalytic site,
329 implicating a phosphorylation-induced global conformational change of MCD as responsible
330 in altering catalytic function. Collectively, our findings demonstrate that phosphorylation
331 modulates decarboxylase-based catalytic function of MCD levering the silkworm-based
332 BmNPV expression system that offers a fail-safe eukaryotic bioengineered protein production
333 platform implementing phosphorylation. Furthermore, authentic recombinant proteins
334 produced from silkworm could be used for functional and structural studies including high-
335 throughput therapeutic drug discovery application.

336 **Note**

337 The authors declare that they have no competing interests.

338 **Acknowledgements**

339 This work was supported partly by the Strategic Young Researcher Overseas Visits Program
340 for Accelerating Brain Circulation from Japan Society for the Promotion of Science (JSPS),
341 Japan, the National Institute of Health, Marriott Heart Disease Research Program, Mayo
342 Clinic. A.T. holds the Marriott Family Professorship in Cardiovascular Diseases Research.

343 **References**

344 An J, Muoio DM, Shiota M, Fujimoto Y, Cline GW, Shulman GI, Koves TR, Stevens R,
345 Millington D, Newgard CB (2004) Hepatic expression of malonyl-CoA decarboxylase
346 reverses muscle, liver and whole-animal insulin resistance. Nat Med 10:268–74. doi:
347 10.1038/nm995

Aparicio D, Pérez-Luque R, Carpena X, Díaz M, Ferrer JC, Loewen PC, Fita I (2013) Structural asymmetry and disulfide bridges among subunits modulate the activity of human malonyl-CoA decarboxylase. J Biol Chem 288:11907–19. doi: 10.1074/jbc.M112.443846

Blom N, Gammeltoft S, Brunak S (1999) Sequence and structure-based prediction of eukaryotic protein phosphorylation sites. J Mol Biol 294:1351–62. doi: 10.1006/jmbi.1999.3310

Bouzakri K, Austin R, Rune A, Lassman ME, Garcia-Roves PM, Berger JP, Krook A, Chibalin A V, Zhang BB, Zierath JR (2008) Malonyl CoenzymeA decarboxylase regulates lipid and glucose metabolism in human skeletal muscle. Diabetes 57:1508–16. doi: 10.2337/db07-0583

Brown GK, Scholem RD, Bankier A, Danks DM (1984) Malonyl coenzyme A decarboxylase deficiency. J Inherit Metab Dis 7:21–6.

Buckner JS, Kolattukudy PE, Poulose AJ (1976) Purification and properties of malonyl-coenzyme A decarboxylase, a regulatory enzyme from the uropygial gland of goose. Arch Biochem Biophys 177:539–51.

Dojima T, Nishina T, Kato T, Uno T, Yagi H, Kato K, Park EY (2009) Comparison of the N-linked glycosylation of human beta1,3-N-acetylglucosaminyltransferase 2 expressed in insect cells and silkworm larvae. J Biotechnol 143:27–33. doi: 10.1016/j.jbiotec.2009.06.013

Du D, Kato T, Suzuki F, Park EY (2009) Expression of protein complex comprising the human prorenin and (pro)renin receptor in silkworm larvae using *Bombyx mori*

370 nucleopolyhedrovirus (BmNPV) bacmids for improving biological function. Mol
371 Biotechnol 43:154–61. doi: 10.1007/s12033-009-9183-7

372 Dyck JR, Barr AJ, Barr RL, Kolattukudy PE, Lopaschuk GD (1998) Characterization of
373 cardiac malonyl-CoA decarboxylase and its putative role in regulating fatty acid
374 oxidation. Am J Physiol 275:H2122–9.

375 Dyck JR, Berthiaume LG, Thomas PD, Kantor PF, Barr AJ, Barr R, Singh D, Hopkins TA,
376 Voilley N, Prentki M, Lopaschuk GD (2000) Characterization of rat liver malonyl-CoA
377 decarboxylase and the study of its role in regulating fatty acid metabolism. Biochem J
378 350 Pt 2:599–608.

379 Dyck JRB, Hopkins TA, Bonnet S, Michelakis ED, Young ME, Watanabe M, Kawase Y,
380 Jishage K, Lopaschuk GD (2006) Absence of malonyl coenzyme A decarboxylase in
381 mice increases cardiac glucose oxidation and protects the heart from ischemic injury.
382 Circulation 114:1721–8. doi: 10.1161/CIRCULATIONAHA.106.642009

383 Folmes CDL, Park S, Terzic A (2013) Lipid metabolism greases the stem cell engine. Cell
384 Metab 17:153–5. doi: 10.1016/j.cmet.2013.01.010

385 Froese DS, Forouhar F, Tran TH, Vollmar M, Kim YS, Lew S, Neely H, Seetharaman J,
386 Shen Y, Xiao R, Acton TB, Everett JK, Cannone G, Puranik S, Savitsky P, Krojer T,
387 Pilka ES, Kiyani W, Lee WH, Marsden BD, von Delft F, Allerston CK, Spagnolo L,
388 Gileadi O, Montelione GT, Oppermann U, Yue WW, Tong L (2013) Crystal structures
389 of malonyl-coenzyme A decarboxylase provide insights into its catalytic mechanism and
390 disease-causing mutations. Structure 21:1182–92. doi: 10.1016/j.str.2013.05.001

Haan EA, Scholem RD, Croll HB, Brown GK (1986) Malonyl coenzyme A decarboxylase deficiency. Clinical and biochemical findings in a second child with a more severe enzyme defect. Eur J Pediatr 144:567–70.

Hwang I-W, Makishima Y, Kato T, Park S, Terzic A, Park EY (2014) Human acetyl-CoA carboxylase 2 expressed in silkworm *Bombyx mori* exhibits posttranslational biotinylation and phosphorylation. Appl Microbiol Biotechnol 98:8201–9. doi: 10.1007/s00253-014-5715-6

Ishikiriyama M, Nishina T, Kato T, Ueda H, Park EY (2009) Human single-chain antibody expression in the hemolymph and fat body of silkworm larvae and pupae using BmNPV bacmids. J Biosci Bioeng 107:67–72. doi: 10.1016/j.jbiosc.2008.11.001

Kamionka M (2011) Engineering of therapeutic proteins production in *Escherichia coli*. Curr Pharm Biotechnol 12:268–74.

Karger AB, Park S, Reyes S, Bienengraeber M, Dyer RB, Terzic A, Alekseev AE (2008) Role for SUR2A ED domain in allosteric coupling within the K(ATP) channel complex. J Gen Physiol 131:185–96. doi: 10.1085/jgp.200709852

Kato T, Kajikawa M, Maenaka K, Park EY (2010) Silkworm expression system as a platform technology in life science. Appl Microbiol Biotechnol 85:459–70. doi: 10.1007/s00253-009-2267-2

Kim KH, López-Casillas F, Bai DH, Luo X, Pape ME (1989) Role of reversible phosphorylation of acetyl-CoA carboxylase in long-chain fatty acid synthesis. FASEB J 3:2250–6.

Kim YS, Kolattukudy PE (1978) Purification and properties of malonyl-CoA decarboxylase from rat liver mitochondria and its immunological comparison with the enzymes from rat brain, heart, and mammary gland. Arch Biochem Biophys 190:234–46.

Kim YS, Kolattukudy PE, Boos A (1979) Malonyl-CoA decarboxylase in rat brain mitochondria. Int J Biochem 10:551–5.

Krawinkel MB, Oldigs HD, Santer R, Lehnert W, Wendel U, Schaub J (1994) Association of malonyl-CoA decarboxylase deficiency and heterozygote state for haemoglobin C disease. J Inherit Metab Dis 17:636–7.

Laurent G, German NJ, Saha AK, de Boer VCJ, Davies M, Koves TR, Dephoure N, Fischer F, Boanca G, Vaitheesvaran B, Lovitch SB, Sharpe AH, Kurland IJ, Steegborn C, Gygi SP, Muoio DM, Ruderman NB, Haigis MC (2013) SIRT4 coordinates the balance between lipid synthesis and catabolism by repressing malonyl CoA decarboxylase. Mol Cell 50:686–98. doi: 10.1016/j.molcel.2013.05.012

Lee GY, Bahk YY, Kim YS (2002) Rat malonyl-CoA decarboxylase; cloning, expression in *E. coli* and its biochemical characterization. J Biochem Mol Biol 35:213–9.

MacPhee GB, Logan RW, Mitchell JS, Howells DW, Tsotsis E, Thorburn DR (1993) Malonyl coenzyme A decarboxylase deficiency. Arch Dis Child 69:433–6.

Matalon R, Michaels K, Kaul R, Whitman V, Rodriguez-Novo J, Goodman S, Thorburn D (1993) Malonic aciduria and cardiomyopathy. J Inherit Metab Dis 16:571–3.

Motohashi T, Shimojima T, Fukagawa T, Maenaka K, Park EY (2005) Efficient large-scale protein production of larvae and pupae of silkworm by *Bombyx mori* nuclear

433 polyhedrosis virus bacmid system. Biochem Biophys Res Commun 326:564–9. doi:
434 10.1016/j.bbrc.2004.11.060

435 Nam HW, Lee GY, Kim YS (2006) Mass spectrometric identification of K210 essential for
436 rat malonyl-CoA decarboxylase catalysis. J Proteome Res 5:1398–406. doi:
437 10.1021/pr050487g

438 Ogata M, Nakajima M, Kato T, Obara T, Yagi H, Kato K, Usui T, Park EY (2009) Synthesis
439 of sialoglycopolypeptide for potentially blocking influenza virus infection using a rat
440 alpha2,6-sialyltransferase expressed in BmNPV bacmid-injected silkworm larvae. BMC
441 Biotechnol 9:54. doi: 10.1186/1472-6750-9-54

442 Otsuki T, Dong J, Kato T, Park EY (2013) Expression, purification and antigenicity of
443 Neospora caninum-antigens using silkworm larvae targeting for subunit vaccines. Vet
444 Parasitol 192:284–7. doi: 10.1016/j.vetpar.2012.09.038

445 Park EY, Abe T, Kato T (2008a) Improved expression of fusion protein using a cysteine-
446 protease- and chitinase-deficient *Bombyx mori* (silkworm) multiple
447 nucleopolyhedrovirus bacmid in silkworm larvae. Biotechnol Appl Biochem 49:135–
448 140. doi: 10.1042/BA20070098

449 Park EY, Kageshima A, Kwon M-S, Kato T (2007) Enhanced production of secretory
450 beta1,3-N-acetylglucosaminyltransferase 2 fusion protein into hemolymph of *Bombyx*
451 *mori* larvae using recombinant BmNPV bacmid integrated signal sequence. J Biotechnol
452 129:681–8. doi: 10.1016/j.jbiotec.2007.01.028

453 Park H, Kaushik VK, Constant S, Prentki M, Przybytkowski E, Ruderman NB, Saha AK
454 (2002) Coordinate regulation of malonyl-CoA decarboxylase, sn-glycerol-3-phosphate

455 acyltransferase, and acetyl-CoA carboxylase by AMP-activated protein kinase in rat
456 tissues in response to exercise. J Biol Chem 277:32571–7. doi:
457 10.1074/jbc.M201692200

458 Park S, Hwang I-W, Makishima Y, Perales-Clemente E, Kato T, Niederländer NJ, Park EY,
459 Terzic A (2013) Spot14/Mig12 heterocomplex sequesters polymerization and restrains
460 catalytic function of human acetyl-CoA carboxylase 2. J Mol Recognit 26:679–88. doi:
461 10.1002/jmr.2313

462 Park S, Lim BBC, Perez-Terzic C, Mer G, Terzic A (2008b) Interaction of asymmetric
463 ABCC9-encoded nucleotide binding domains determines KATP channel SUR2A
464 catalytic activity. J Proteome Res 7:1721–8. doi: 10.1021/pr7007847

465 Pender C, Trentadue AR, Pories WJ, Dohm GL, Houmard JA, Youngren JF (2006)
466 Expression of genes regulating Malonyl-CoA in human skeletal muscle. J Cell Biochem
467 99:860–867. doi: 10.1002/jcb.20944

468 Saggerson D (2008) Malonyl-CoA, a key signaling molecule in mammalian cells. Annu Rev
469 Nutr 28:253–72. doi: 10.1146/annurev.nutr.28.061807.155434

470 Saha AK, Schwarsin AJ, Roduit R, Masse F, Kaushik V, Tornheim K, Prentki M, Ruderman
471 NB (2000) Activation of malonyl-CoA decarboxylase in rat skeletal muscle by
472 contraction and the AMP-activated protein kinase activator 5-aminoimidazole-4-
473 carboxamide-1-beta -D-ribofuranoside. J Biol Chem 275:24279–83. doi:
474 10.1074/jbc.C000291200

475 Sambandam N, Steinmetz M, Chu A, Altarejos JY, Dyck JRB, Lopaschuk GD (2004)
476 Malonyl-CoA decarboxylase (MCD) is differentially regulated in subcellular

477 compartments by 5'AMP-activated protein kinase (AMPK). Studies using H9c2 cells
478 overexpressing MCD and AMPK by adenoviral gene transfer technique. Eur J Biochem
479 271:2831–40. doi: 10.1111/j.1432-1033.2004.04218.x

480 Samokhvalov V, Ussher JR, Fillmore N, Armstrong IKG, Keung W, Moroz D, Lopaschuk
481 DG, Seubert J, Lopaschuk GD (2012) Inhibition of malonyl-CoA decarboxylase reduces
482 the inflammatory response associated with insulin resistance. Am J Physiol Endocrinol
483 Metab 303:E1459–68. doi: 10.1152/ajpendo.00018.2012

484 Scholte HR (1969) The intracellular and intramitochondrial distribution of malonyl-CoA
485 decarboxylase and propionyl-CoA carboxylase in rat liver. Biochim Biophys Acta
486 178:137–44.

487 Voilley N, Roduit R, Vicaretti R, Bonny C, Waeber G, Dyck JR, Lopaschuk GD, Prentki M
488 (1999) Cloning and expression of rat pancreatic beta-cell malonyl-CoA decarboxylase.
489 Biochem J 340 (Pt 1:213–7.

490 Xue J, Peng J, Zhou M, Zhong L, Yin F, Liang D, Wu L (2012) Novel compound
491 heterozygous mutation of MLYCD in a Chinese patient with malonic aciduria. Mol
492 Genet Metab 105:79–83. doi: 10.1016/j.ymgme.2011.09.007

493 Yano S, Sweetman L, Thorburn DR, Mofidi S, Williams JC (1997) A new case of malonyl
494 coenzyme A decarboxylase deficiency presenting with cardiomyopathy. Eur J Pediatr
495 156:382–3.

496 Zhou D, Yuen P, Chu D, Thon V, McConnell S, Brown S, Tsang A, Pena M, Russell A,
497 Cheng J-F, Nadzan AM, Barbosa MS, Dyck JRB, Lopaschuk GD, Yang G (2004)

498 Expression, purification, and characterization of human malonyl-CoA decarboxylase.
499 Protein Expr Purif 34:261–9. doi: 10.1016/j.pep.2003.11.023

500

Figure and Table Legends

Fig. 1 A **s**chematic diagram of recombinant Δ39aa-hMCD bacmid construction and expression in silkworm. The Δ39aa-hMCD gene was amplified by PCR. This PCR fragment was digested by restriction enzymes and ligated into pFastbac1 vector. The pFastbac-Δ39aa-hMCD was transformed into *E. coli* BmDH10Bac harboring cysteine protease- and chitinase-deficient *Bombyx mori* nucleopolyhedrovirus (BmNPV-*CP*⁻-*Chi*⁻). The constructed recombinant bacmid was directly injected into the dorsum of the larvae on the first day of their fifth-instar and pupae. M, mitochondrial-targeting sequence; K, Kozak sequence; F, FLAG tag; SKL, peroxisomal-targeting sequence. Black and green arrows denote bacmid constructions for Δ39aa-hMCD and for Δ39aa-hMCD mutants, respectively.

Fig. 2 SDS-PAGE (A) and Western blot (B) of recombinant Δ39aa-hMCD expressed in silkworm fat body and pupae. MW, molecular weight markers; FB, Δ39aa-hMCD from fat body; P, Δ39aa-hMCD from pupae. Protein in homogenate was extracted with lysis buffer and purified by anti-FLAG M2 affinity gel column. Mock sample indicates bacmid, without hMCD gene, injected silkworm. An anti-FLAG M2 and an anti mouse IgG-HRP were used to detect Δ39aa-hMCD, and an anti-phosphoserine antibody was used to detect phosphorylation of Δ39aa-hMCD.

Fig. 3 Amino acid sequence alignments of human, rat and mouse MCD. (A). Blue, two initiating methionines; Red, putative phosphorylation site residues of hMCD by Netphos 2.0 prediction server; Arrow, point mutation sites for dephosphorylation of hMCD in this study. (B) Predicted phosphorylation sites of hMCD. Prediction score is the probability of phosphorylation (*max* = 1). (C) A point mutation in hMCD replaced serine (S) 204 (codon

524 TCA) with glycine (G) (codon GGA) and tyrosine (Y) 405 (codon TAC) with phenylalanine
525 (F) (codon TTC).

526 **Fig. 4** Western blot of purified Δ39aa-hMCD and their mutants. MW, molecular weight
527 markers; WT, wild type Δ39aa-hMCD; S204G, mutated Δ39aa-hMCD at Serine 204; Y405F,
528 mutated Δ39aa-hMCD at Tyrosine 405; FB and P denote proteins purified from fat body and
529 pupae, respectively. A monoclonal anti-phosphoserine and anti-phosphotyrosine antibodies
530 produced in mouse were used as primary antibodies, and anti-mouse IgG-HRP was used as a
531 secondary antibody. In western blot, 5 μg of proteins per well were used.

532 **Fig. 5** Molecular organization of human peroxisomal MCD (PDB accession number: 2YGW).
533 (A) A cartoon representation of MCD monomer composed of an N-terminal helical domain
534 and a C-terminal catalytic domain where the catalytic acetyl-CoA binding site is located. (B)
535 Structural arrangement of MCD tetramer. Inter-subunit disulfide bridges, Cys-206—Cys-206
536 in red spheres and Cys-243—Cys-243 in blue spheres, link the four subunits of tetramer. (C)
537 MCD with phosphorylated residues of Ser-204 and Tyr-405. Cys-206 connects two subunits
538 through the disulfide bond. (D) Tyr-405, located in the vicinity of the catalytic dyad of Ser-
539 329 and His-423, forms a hydrogen bond with Asn-417. Cartoon MCD structures were
540 generated with PyMol.

541 **Table 1.** The yields of recombinant proteins from silkworm larva or pupa

542 **Table 2.** Purification of Δ39aa-hMCD from silkworm fat body and pupae

543 **Table 3.** Specific activities of purified Δ39aa-hMCD mutants from silkworm fat body and
544 pupae

545

546

Table 1. The yields of recombinant proteins from silkworm larva or pupa

Protein	μg/larva	μg/pupa	Reference
GFPuv-β3GnT2	91		Park et al. 2007
Anti-BSA scFv	188		Ishikiriyama et al. 2009
ST6Gal1	220		Ogata et al. 2009
SAG1	170		Otsuki et al. 2013
SRS2	20		Otsuki et al. 2013
ACC2	150		Park et al. 2013
ACC2		500	Hwang et al. 2014
MCD	119	344	In this study

GFP, green fluorescent protein; β3GnT2, beta1,3-N-acetylglucosaminyl transferase 2; scFv, Human single-chain Fv fragment; ST6Gal1, rat alpha2,6-sialyltransferase; SAG1, *N. caninum* surface antigen 1; SRS2, SAG1-related sequence 2; ACC2, acetyl-CoA carboxylase 2; MCD, malonyl-CoA decarboxylase.

547

548

Table 2. Purification of **Δ39aa-hMCD** from silkworm fat body and pupae

	Volume (mL/silkworm)	Protein (mg/silkworm)	Specific activity (nmol/mg/min)	Relative activity
Fat body				
Homogenate	3	193	19.61 ± 3.96	1
Purified Δ39aa-hMCD	0.5	0.119	59.54 ± 7.68	3
Pupae				
Homogenate	3	232	12.81 ± 3.36	1
Purified Δ39aa-hMCD	0.5	0.344	48.16 ± 7.89	3.7

549

Table 3. Specific activities of purified Δ39aa-hMCD mutants from silkworm fat body and pupae

	Specific activity (nmol/mg/min)	Relative activity
Fat body		
Δ39aa-hMCD	59.54 ± 7.68	1
S204G	30.36 ± 2.25	0.51
Y405F	33.45 ± 3.56	0.56
Pupae		
Δ39aa-hMCD	48.16 ± 7.89	1
S204G	24.37 ± 1.99	0.51
Y405F	31.24 ± 1.69	0.64

550

551

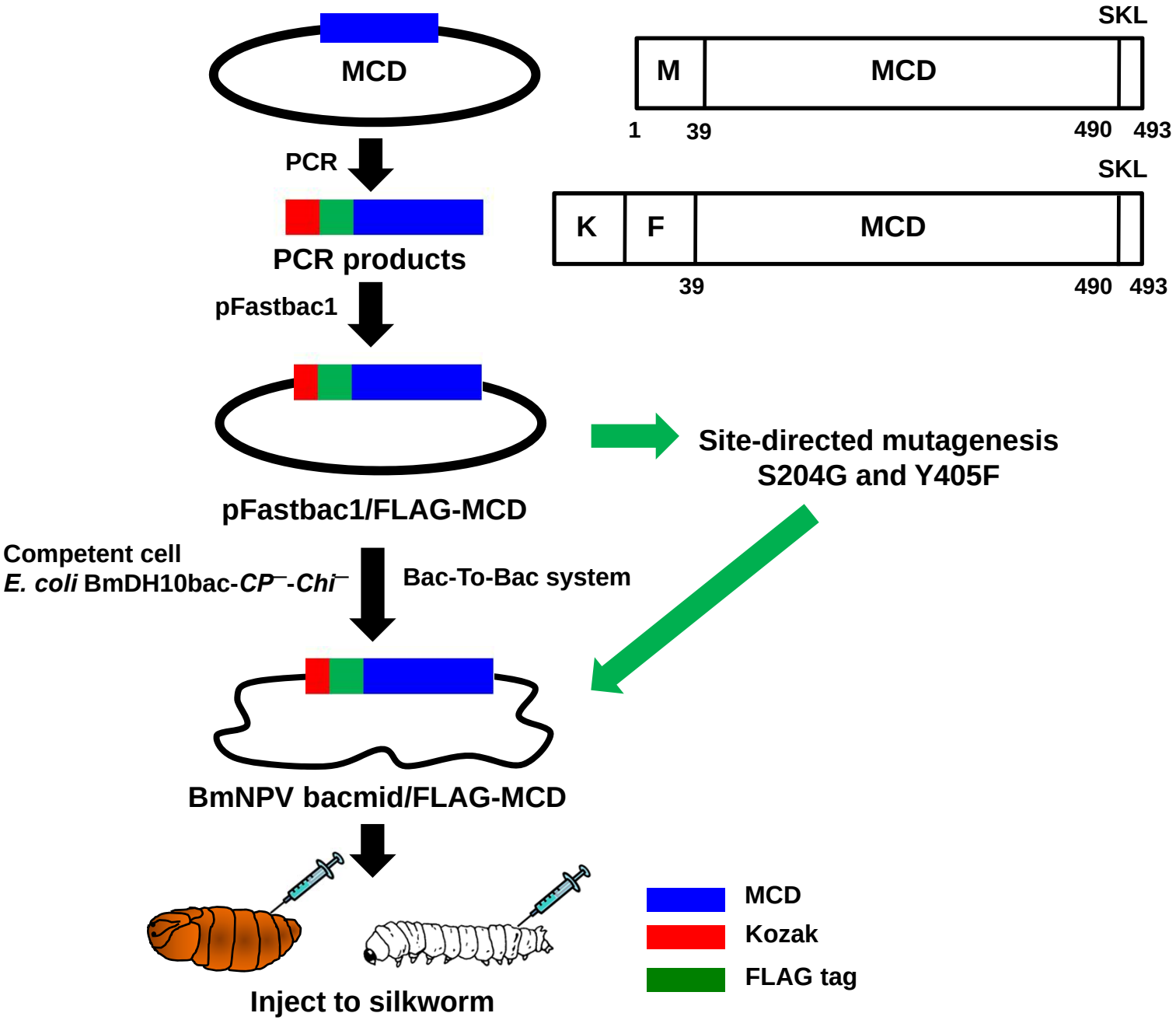
MCD
PCR
PCR products
pFastbac1
pFastbac1/FLAG-MCD
Site-directed mutagenesis
S204G and Y405F
Competent cell
E. coli BmDH10bac-CP⁻-Chi⁻
Bac-To-Bac system
BmNPV bacmid/FLAG-MCD
Inject to silkworm
SKL
M
MCD
1
39
490
493
SKL
K
F
MCD
39
490
493
MCD
Kozak
FLAG tag

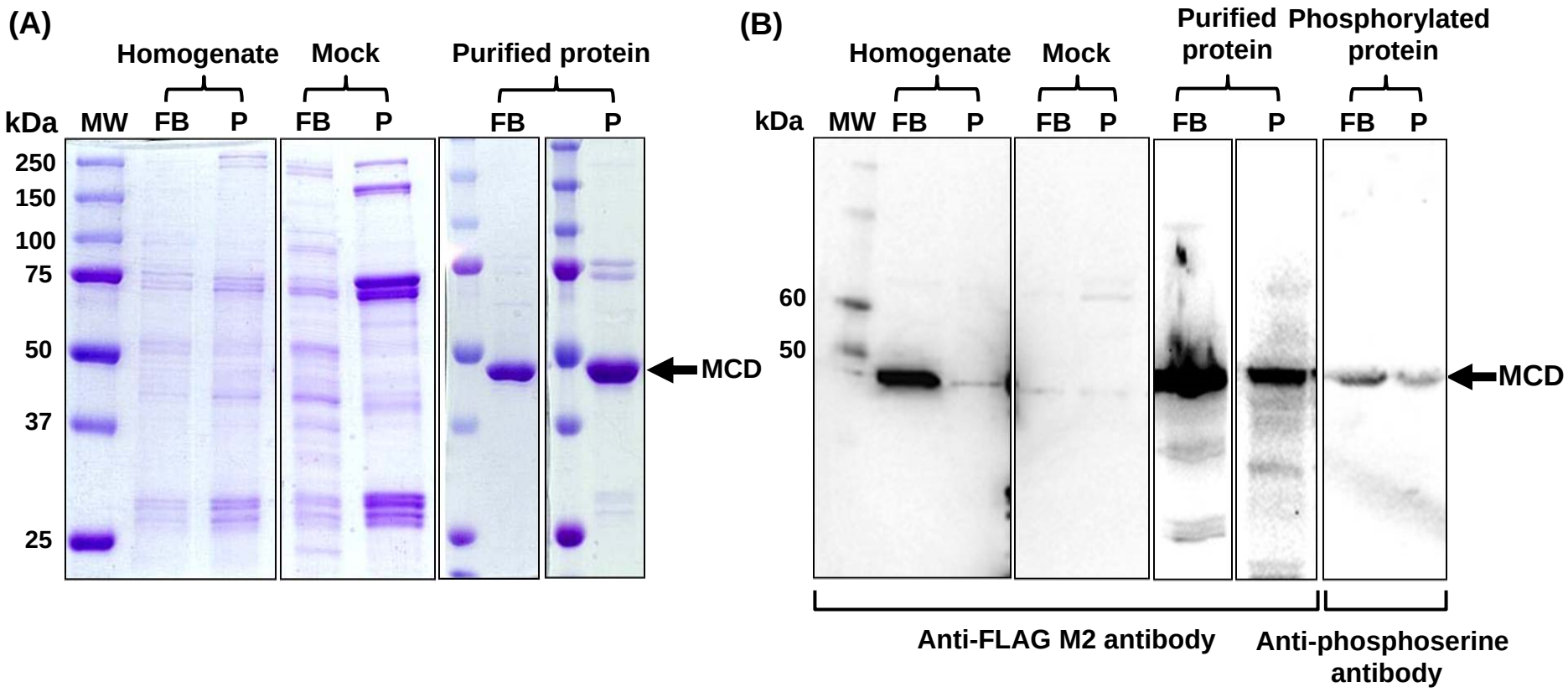
(A)
Homogenate
Mock
Purified protein
kDa
MW
FB
P
FB
P
FB
P
250
150
100
75
50
37
25
MCD
(B)
Homogenate
Mock
Purified protein
Phosphorylated protein
kDa
MW
FB
P
FB
P
FB
P
FB
P
60
50
MCD
Anti-FLAG M2 antibody
Anti-phosphoserine antibody

(A)

```
HUMAN MRGFGPGLTARRLLPLRLPPRPPGPRLASGQAAGALERAMDELLRRAVPPTPAYELREKT 60
RAT   MRGLGPSLRARRLLPLRYPPRPPGPRGPR-LCSGLTASAMDELLRRAVPPTPAYELREKT 59
MOUSE MRGLGPGLRARRLLPLRSPPRPPGPRGRR-LCGGLAASAMDELLRRAVPPTPAYELREKT 59
      ***:**.* ******** ********     ..*    **********************
HUMAN PAPAEGQCADFVSFYGGLAETAQRAELLGRLARGFGVDHGQVAEQSAGVLHLRQQQREAA 120
RAT   PAPAEGQCADFVSFYGGLAEAAQRAELLGRLAQGFGVDHGQVAEQSAGVLQLRQQSREAA 119
MOUSE PAPAEGQCADFVSFYGGLAEASQRAELLGRLAQGFGVDHGQVAEQSAGVLQLRQQAREAA 119
      ********************::*********:*****************:**** ****
HUMAN VLLQAEDRLRYALVPRYRGLFHHISKLDGGVRFLVQLRADLLEAQALKLVEGPDVREMNG 180
RAT   VLLQAEDRLRYALVPRYRGLFHHISKLDGGVRFLVQLRADLLEAQALKLVEGPHVREMNG 179
MOUSE VLLQAEDRLRYALVPRYRGLFHHISKLDGGVRFLVQLRADLLEAQALKLVEGPHVREMNG 179
      ****************************************************.******

HUMAN VLKGMLSEWFSSGFLNLERVTWHSPCEVLQKISEAEAVHPVKNWMDMKRRVGPYRRCYFF 240
RAT   VLKSMLSEWFSSGFLNLERVTWHSPCEVLQKISECEAVHPVKNWMDMKRRVGPYRRCYFF 239
MOUSE VLKSMLSEWFSSGFLNLERVTWHSPCEVLQKISECEAVHPVKNWMDMKRRVGPYRRCYFF 239
      ***.******************************.************************
HUMAN SHCSTPGEPLVVLHVALTGDISSNIQAIVKEHPPSETEEKNKITAAIFYSISLTQQGLQG 300
RAT   SHCSTPGDPLVVLHVALTGDISNNIQSIVKECPPSETEEKNRIAAAVFYSISLTQQGLQG 299
MOUSE SHCSTPGEPLVVLHVALTGDISNNIQGIVKECPPTETEERNRIAAAIFYSISLTQQGLQG 299
      *******:**************.***.**** **:****:*:*:**:*************
HUMAN VELGTFLIKRVVKELQREFPHLGVFSSLSPIPGFTKWLLGLLNSQTKEHGRNELFTDSEC 360
RAT   VELGTFLIKRVVKELQKEFPHLGAFSSLSPIPGFTKWLLGLLNVQGKEYGRNELFTDSEC 359
MOUSE VELGTFLIKRVVKELQKEFPQLGAFSSLSPIPGFTKWLLGLLNVQGKEHGRNELFTDSEC 359
      ****************:***:**.****************** * **:***********

HUMAN KEISEITGGPINETLKLLLSSSEWVQSEKLVRALQTPLMRLCAWYLYGEKHRGYALNPVA 420
RAT   KEIAEVTGDPVHESLKGLLSSGEWAKSEKLAQALQGPLMRLCAWYLYGEKHRGYALNPVA 419
MOUSE QEISAVTGNPVHESLKGFLSSGEWVKSEKLTQALQGPLMRLCAWYLYGEKHRGYALNPVA 419
      :**: :** *:.*:** :***.**.:****.:*** ************************
HUMAN NFHLQNGAVLWRINWMADVSLRGITGSCGLMANYRYFLEETGPNSTSYLGSKIIKASEQV 480
RAT   NFHLQNGAVMWRINWMADSSLKGLTSSCGLMVNYRYYLEETGPNSISYLGSKNIKASEQI 479
MOUSE NFHLQNGAVMWRINWMADSSLKGLTSSCGLMVNYRYYLEETGPNSISYLGSKNIKASEQI 479
      *********:******** **:*:*.*****.****:******** ****** ******:
HUMAN LSLVAQFQKNSKL 493
RAT   LSLVAQFQSNSKL 492
MOUSE LSLVAQFQNNSKL 492
      ********.****
```

(B)

Amino acid	Prediction Score
Ser204	0.980
Ser275	0.997
Ser329	0.905
Ser380	0.791
Thr9	0.893
Thr60	0.982
Thr245	0.869
Thr396	0.772
Tyr468	0.541

(C)

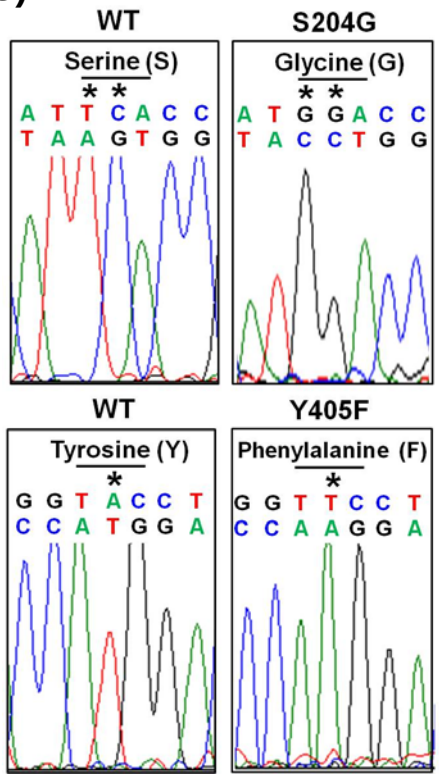

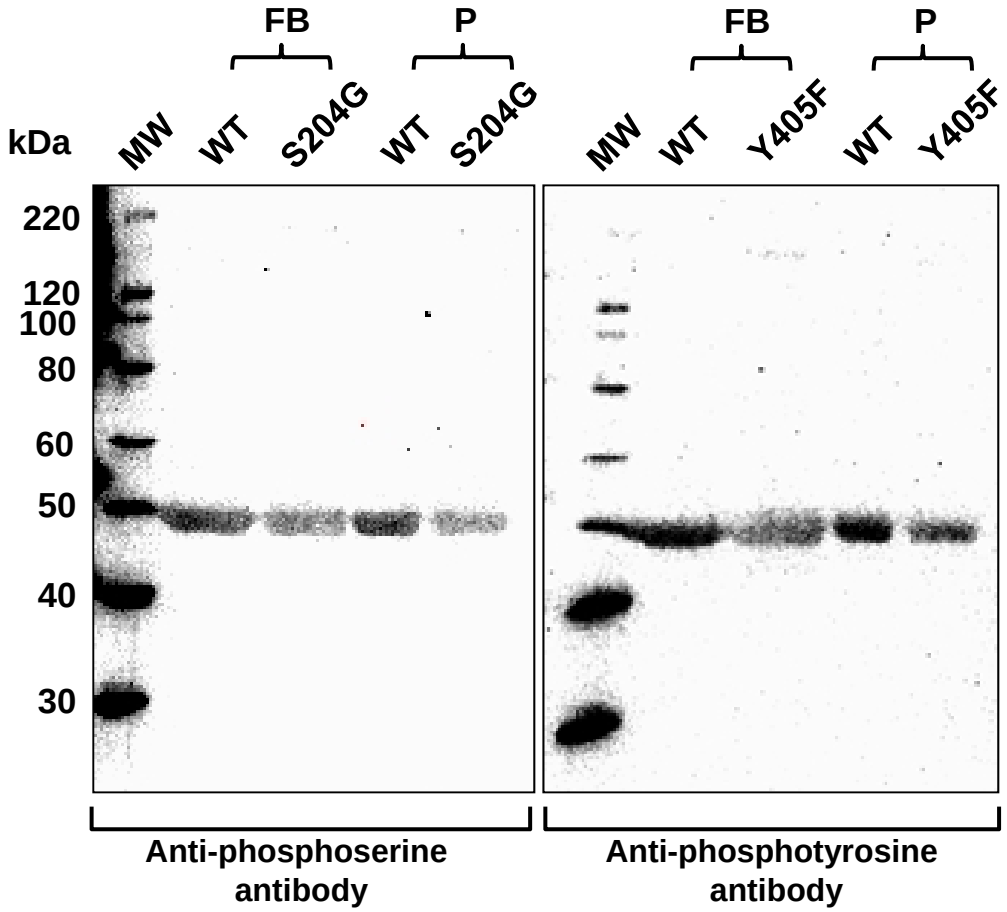
FB
P
FB
P
kDa
MW
WT
S204G
WT
S204G
MW
WT
Y405F
WT
Y405F
220
120
100
80
60
50
40
30
Anti-phosphoserine antibody
Anti-phosphotyrosine antibody

Hwang et al.. Fig. 5

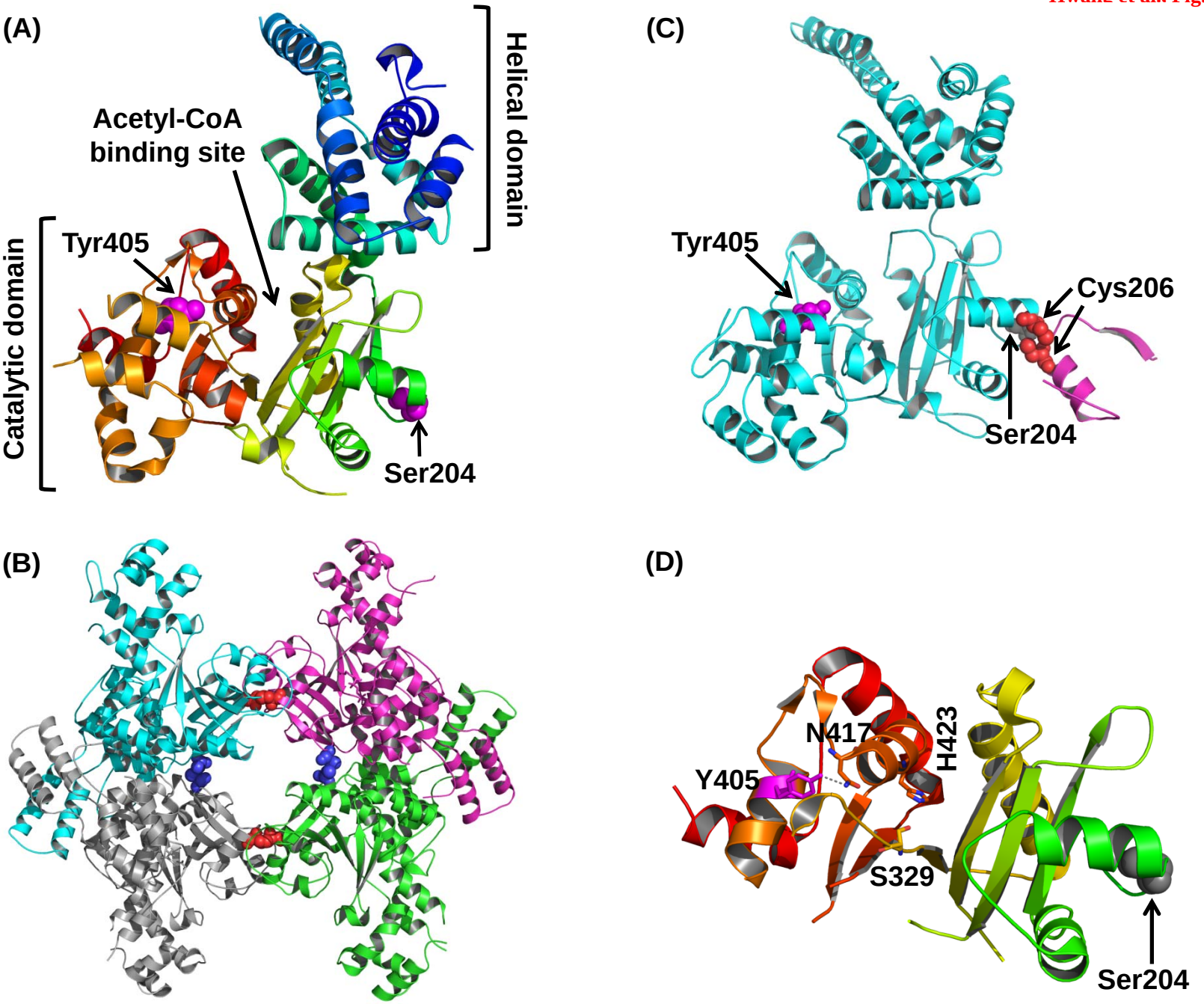

Applied Microbiology and Biotechnology

Supporting information

Phosphorylation of Ser-204 and Tyr-405 in human malonyl-CoA decarboxylase expressed in silkworm *Bombyx mori* regulates catalytic decarboxylase activity

In-Wook Hwang · Yu Makishima · Tomohiro Suzuki · Tatsuya Kato · Sungjo Park · Andre Terzic · Shin-kyo Chung · Enoch Y. Park

---

In-Wook Hwang · Enoch Y. Park (✉)
Laboratory of Biotechnology, Integrated Bioscience Section, Graduate School of Science and Technology, Shizuoka University, 836 Ohya, Suruga-ku, Shizuoka, 422-8529, Japan. E-mail: park.enoch@shizuoka.ac.jp; Tel. & Fax: +81-54-2384887

Yu Makishima · Tatsuya Kato · Enoch Y. Park

Laboratory of Biotechnology, Department of Applied Biological Chemistry, Faculty of Agriculture, Shizuoka University, 836 Ohya, Suruga-ku, Shizuoka, 422-8529, Japan.

Tomohiro Suzuki

Research Institute of Green Science and Technology, Shizuoka University, 836 Ohya Suruga-ku, Shizuoka, 422-8529, Japan.

Tatsuya Kato · Enoch Y. Park

Laboratory of Biotechnology, Green Chemistry Research Division, Research Institute of Green Science and Technology, Shizuoka University, 836 Ohya Suruga-ku, Shizuoka, 422-8529, Japan.

Sungjo Park · Andre Terzic

Center for Regenerative Medicine, Mayo Clinic, 200 First Street SW, Rochester, MN, 55905, USA. Marriott Heart Disease Research Program, Division of Cardiovascular Diseases, Departments of Medicine, Molecular Pharmacology and Experimental Therapeutics, and Medical Genetics, Mayo Clinic, 200 First Street SW, Rochester, MN, 55905, USA.

Shin-kyo Chung

School of Food Science and Biotechnology, Kyungpook National University, Daegu 702-701, Republic of Korea

Authors' E-mail address;
In-Wook Hwang: gunryung21@hanmail.net (IH)
Yu Makishima: mmm.yu@live.jp (YM)
Tomohiro Suzuki: atsuzuk@ipc.shizuoka.ac.jp (TS)
Tatsuya Kato: atkato@ipc.shizuoka.ac.jp (TK)
Sungjo Park: park.sungjo@mayo.edu (SP)
Andre Terzic: terzic.andre@mayo.edu (AT)
Shin-kyo Chung: kchung@knu.ac.kr (SC)
Enoch Y. Park: park.enoch@shizuoka.ac.jp (EYP)

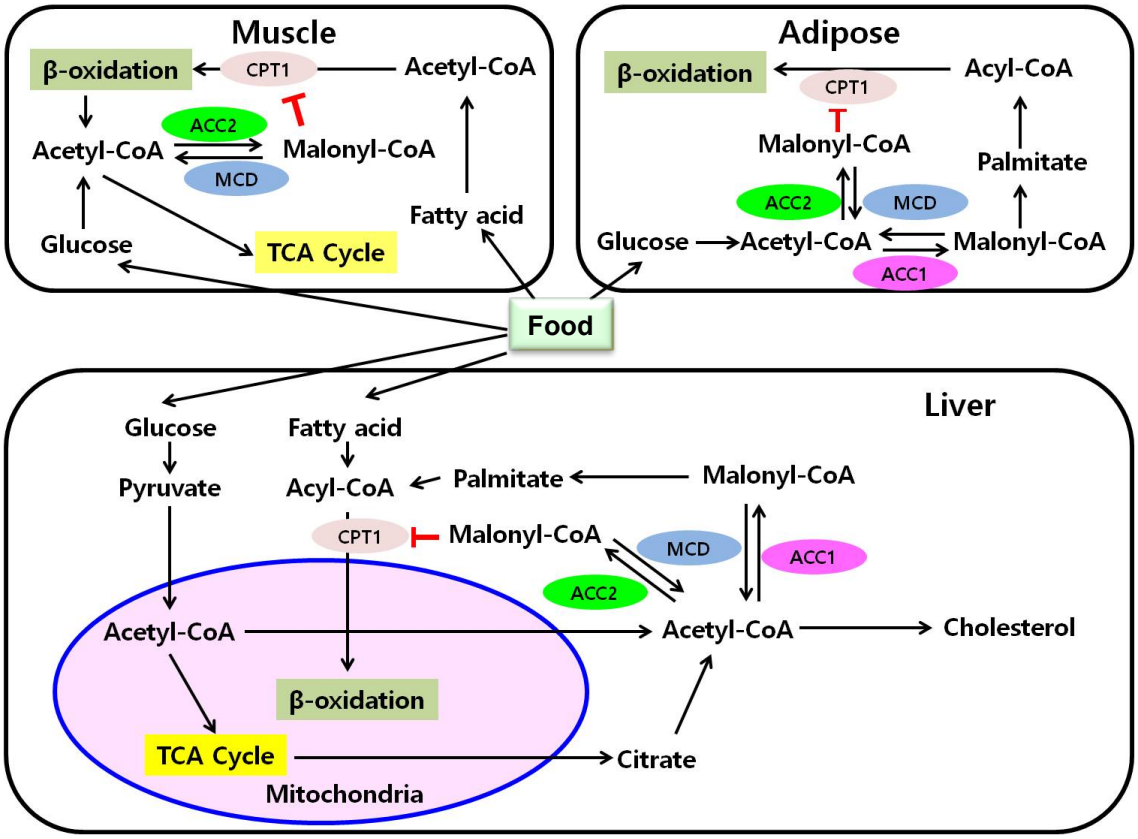

Figure S1. Malonyl-CoA decarboxylase (MCD) plays essential roles in lipid metabolism with acetyl-CoA carboxylase 1 and 2 (ACC1 and ACC2) by modulating the acetyl-CoA and malonyl-CoA in muscle, adipose and liver tissues. MCD catalyzes the conversion of malonyl-CoA to acetyl-CoA. The malonyl-CoA is an intermediate metabolite for fatty acid synthesis and acts as an inhibitor of carnitine palmitoyl transferase 1 (CPT-1) for fatty acid β-oxidation. Thus, MCD modulates the lipid metabolism by regulation of malonyl-CoA levels. Modified from Wakil and Abu-Elheiga, 2009.

Reference

Salih J. Wakil and Lutfi A. Abu-Elheiga, Fatty acid metabolism: target for metabolic syndrome, S138–S143 (2009).

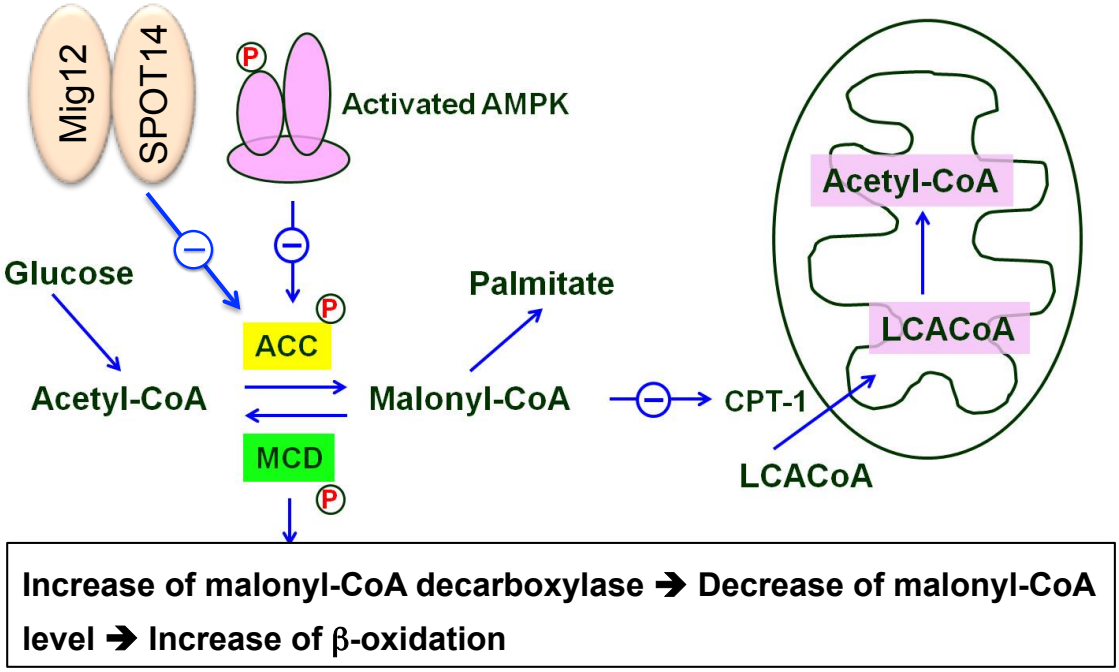

Figure S2. A proposed model of malonyl-CoA decarboxylase (MCD) phosphorylation in regulating lipid metabolism. Phosphorylation of Ser-204 and Tyr-405 in MCD enhances malonyl-CoA decarboxylation by reducing malonyl-CoA levels in cytoplasm, which promotes a stimulation of long chain acryl-CoA (LCACoA) oxidation by releasing the malonyl-CoA inhibition of carnitine palmitoyl transferase 1 (CPT1). In addition to MCD dependent regulation, phosphorylation of acetyl-CoA carboxylase (ACC) by AMP-activated kinase (AMPK) or inhibition of ACC by Spot14/Mig12 diminishes malonyl-CoA levels, subsequently promoting lipid oxidation.

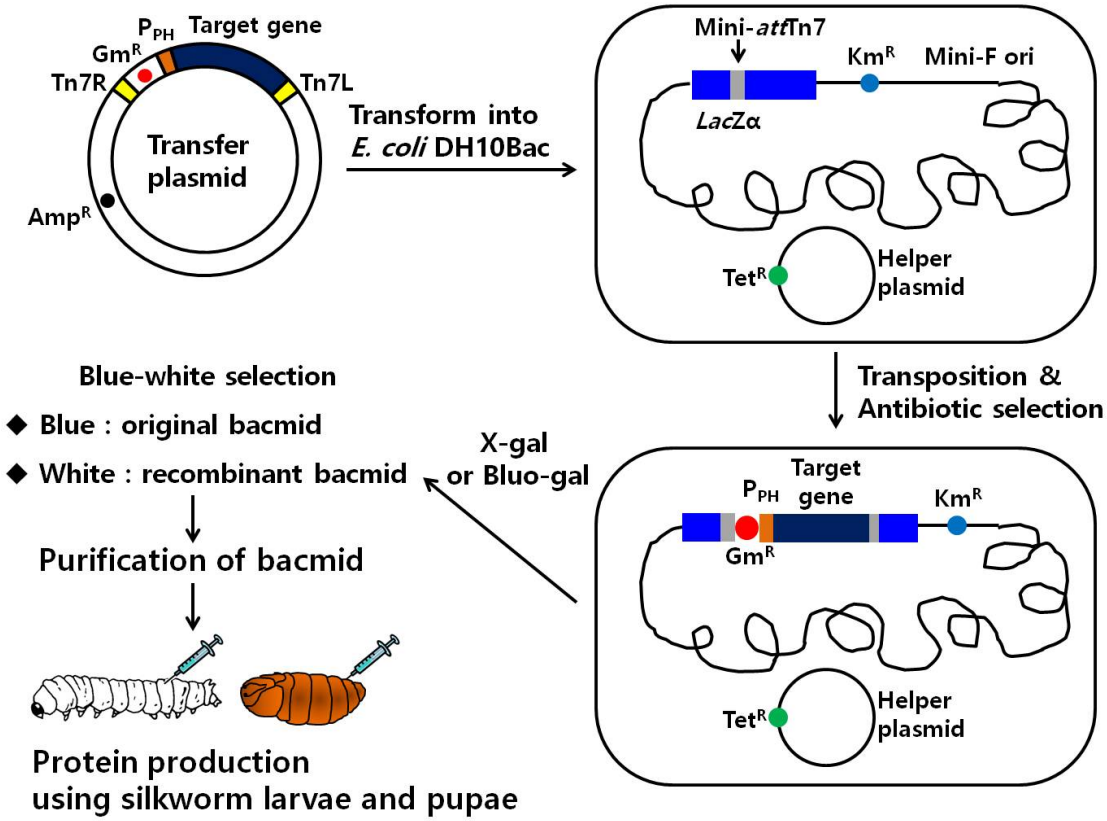

Figure S3. Construction of recombinant bacmid by Bac-to-Bac system and protein production using silkworms. Amp^R; Ampiciliin resistance, Gm^R; Gentamycin resistance, Km^R; kanamycin resistance, Tet^R; tetracycline resistance, P_{PH}; polyhedrin promoter.